EVOLUTION IN OFF-CRITICAL DIBLOCK COPOLYMER MELTS

Michael Helmers

Mathematical Institute, University of Oxford
24-29 St Giles', Oxford, OX1 3LB, United Kingdom

Barbara Niethammer

Mathematical Institute, University of Oxford
24-29 St Giles', Oxford, OX1 3LB, United Kingdom

Xiaofeng Ren

Department of Mathematics, The George Washington University
2115 G Street, Washington, DC 20052, USA

Abstract. We study the evolution of diblock copolymer melts in which one component has small volume fraction. In this case one observes phase morphologies which consist of small spheres of the minority component embedded in the other component. Based on the Ohta-Kawasaki free energy one can set up an evolution equation which has the interpretation of a gradient flow. We restrict this gradient flow to morphologies in which the minority phase consists of spheres and derive monopole approximations for different parameter regimes. We use these approximations for simulations of large particle systems.

1. **Introduction.**

1.1. **Diblock copolymers.** A diblock copolymer molecule is a linear sub-chain of N_A A-monomers grafted covalently to another sub-chain of N_B B-monomers. Because of the repulsion between the unlike monomers, the different type sub-chains tend to segregate, but as they are chemically bonded in chain molecules, segregation of sub-chains cannot lead to a macroscopic phase separation. Only a local micro-phase separation occurs: micro-domains rich in A and B emerge. These micro-domains form morphology patterns on a larger scale. In this paper we are mainly interested in the case that the fraction of, say, A-monomers in a chain is small. Then we observe patterns which consist of many small separated spheres rich in A-monomers.

1.2. **The Ohta-Kawasaki free energy.** The Ohta-Kawasaki [11] free energy of an incompressible diblock copolymer melt is a functional of the A-monomer density field. Let $u(x)$ be the relative A-monomer number density at a point x in the sample. When there is high A-monomer concentration at x, $u(x)$ is close to 1; when there is high concentration of B-monomers at x, $u(x)$ is close to 0. A value of $u(x)$

2000 *Mathematics Subject Classification.* 82C26, 82D60, 37M05.

Key words and phrases. Diblock copolymers, gradient flow, monopole approximation.

between 0 and 1 means that a mixture of A- and B-monomers occupies x. The free energy of the system is written as

$$I_\eta(u) := \int_D \left(\frac{\eta}{2} |\nabla u|^2 + \frac{1}{\eta} W(u) + \frac{\gamma}{2} |(-\Delta)^{-1/2}(u-\rho)|^2 \right) dx,$$

defined in $X_a = \{u \in W^{1,2}(D) : \frac{1}{|D|} \int_D u = \rho\}$.

When the free energy I_η is minimized, the three terms of the integrand (the energy density of the material) have different preferences. The first term likes large blocks of monomers, thereby reducing the total size of the interface between the two monomers. The function W in the second term is a double well potential with two global minima at 0 and 1, reflecting its preference for segregated monomers over mixtures. The third nonlocal term is minimized if $u \equiv \rho$. However, this configuration of u makes the second term large. The second best choice for the third term is to have u oscillate rapidly around ρ. This way, because of the compact nature of $(-\Delta)^{-1/2}$ (when D is bounded), $(-\Delta)^{-1/2}(u-\rho)$ becomes close to 0 and hence the third term becomes small. As these preferences compete and compromise, small blocks rich in A-monomers and B-monomers appear. This phenomenon is known as micro-phase separation. For a further analysis of the scaling of the energy we refer to [4].

1.3. **The sharp interface limit.** If η is small the interfacial regions become smaller and one can replace I_η by its sharp interface limit. In [10] the Ohta-Kawasaki theory is formulated on a bounded domain as a singularly perturbed variational problem with a nonlocal term and the limiting sharp interface problem is identified. The latter is rigorously derived in [12] as a Γ-limit of the singularly perturbed variational problem.

In this paper we consider an idealized situation, in which $D = \mathbb{R}^3$, so we formulate the energy directly for this case. The corresponding energy is defined for all $\Omega \in \mathbb{R}^3$ with $|\Omega| = \rho$ and is given by

$$E(\Omega) = \mathcal{H}^2(\partial\Omega) + \frac{\gamma}{2} \int_{\mathbb{R}^3} \left| (-\Delta)^{-1/2}\chi \right|^2 dx, \tag{1}$$

where χ is the characteristic function of Ω and $\int_{\mathbb{R}^3} \left| (-\Delta)^{-1/2}\chi \right|^2 dx = \int_{\mathbb{R}^3} |\nabla\mu|^2 dx$ with $-\Delta\mu = \chi$ in $\mathbb{R}^3$.

1.4. **A time dependent model.** We are interested in how an initial configuration of a diblock copolymer melt evolves towards a state of minimal energy. An appropriate evolutionary model set in whole space which reduces E and keeps the volume fraction of both phases conserved is the following Mullins-Sekerka type free boundary problem. In this model the normal velocity v of the interface $\partial\Omega = \partial\Omega(t)$ is given by

$$v = [\nabla u \cdot \vec{n}] \qquad \text{on } \partial\Omega, \tag{2}$$

where $[\nabla u \cdot \vec{n}]$ denotes the jump of the normal component of the gradient across the interface. (Here $\vec{n}$ denotes the outer normal to Ω and $[f] = \lim_{x \notin \Omega, x \to \partial\Omega} f(x) - \lim_{x \in \Omega, x \to \partial\Omega} f(x)$.) The potential u is for each time determined via

$$-\Delta u = 0 \qquad \text{in } \mathbb{R}^3 \backslash \partial\Omega, \tag{3}$$

$$u = \kappa + \gamma(-\Delta)^{-1}\chi \quad \text{on } \partial\Omega \tag{4}$$

with no-flux boundary conditions for u at infinity. Aspects of a local well-posedness theory for the Mullins-Sekerka model (that is the case $\gamma = 0$) can be found for example in [2], [3] and [6].

1.5. **The gradient flow structure of the evolutionary model.** The evolution defined by (2)-(4) has an interpretation as a gradient flow on a Riemannian manifold, more precisely it is the gradient flow of the energy (1) with respect to the H^{-1} norm in the bulk. To reveal this structure consider the manifold $\mathcal{M} := \{\Omega \subset \mathbb{R}^3 \,|\, |\Omega| = \rho\}$ of all subsets of $\mathbb{R}^3$ with fixed volume. The tangent space $T_\Omega \mathcal{M}$ at an element $\Omega \in \mathcal{M}$ is described by all kinematically admissible normal velocities of $\partial\Omega$, that is,

$$T_\Omega \mathcal{M} = \left\{ v \colon \partial\Omega \to \mathbb{R} \,\Big|\, \int_{\partial\Omega} v \, dS = 0 \right\}.$$

The metric tensor on the tangent space is given by

$$g_\Omega(v^1, v^2) = \int_{\mathbb{R}^3} \nabla u^1 \cdot \nabla u^2 \, dx,$$

where u^α solves

$$-\Delta u^\alpha = 0 \quad \text{in } \mathbb{R}^3 \backslash \partial\Omega,$$
$$[\nabla u^\alpha \cdot \vec{n}] = v^\alpha \quad \text{on } \partial\Omega.$$

Note that u^α is well-defined up to an additive constant (see [5] for a rigorous set-up).

The gradient flow of the energy (1) is now the dynamical system where at each time the velocity is the element of the tangent space which points in the direction of steepest descent of the energy. In other words, v is such that

$$g_{\Omega(t)}(v, \tilde{v}) = -\langle DE(\Omega(t)), \tilde{v} \rangle \tag{5}$$

for all $\tilde{v} \in T_{\Omega(t)} \mathcal{M}$. Choosing $\tilde{v} = v$ we immediately obtain the energy estimate associated with each gradient flow, which is

$$\int_0^T g_{\Omega(t)}(v, v) \, dt + E(\Omega(T)) = E(\Omega(0))$$

for all $T > 0$.

It is well known that the first variation of the surface energy, the first summand of E, is the mean curvature. The second nonlocal part is given by $\frac{1}{2} \int_{\mathbb{R}^3} |\nabla\mu|^2 \, dx$, where μ solves $-\Delta\mu = \chi$. Hence $\int_{\mathbb{R}^3} |\nabla\mu|^2 \, dx = \int_{\mathbb{R}^3} \mu\chi \, dx = \int_\Omega \mu \, dx$ and the first variation in direction $\tilde{v} \in T_\Omega \mathcal{M}$ is given by $\int_{\partial\Omega} \mu\tilde{v} \, dS$. Thus (5) reads after an integration by parts in the metric tensor

$$\int_{\partial\Omega} u\tilde{v} \, dS = \int_{\partial\Omega} (\kappa + \gamma\mu)\tilde{v} \, dS$$

for all $\tilde{v} \in T_{\Omega(t)} \mathcal{M}$. This is up to an irrelevant constant just (4).

The advantage of the gradient flow perspective is that it can be restricted in a natural way to a lower dimensional submanifold. We will make use of this idea in the next section.

2. Reduced models.

2.1. **Off-critical mixtures and restriction to spherical particles.** In the following we are interested in the regime where the fraction of A-monomers is much smaller than the one of B-monomers. In this case the A-phase consists of a set of many small disconnected approximately spherical particles. In view of this fact it seems natural to restrict the evolution (2)-(4) to spherical particles by restricting the gradient flow to such morphologies. For the case $\gamma = 0$ it has been shown rigorously in [1] that such an approximation is valid. We also refer to [13], in which stable states of the energy are established which consist of a collection of spheres.

We define the submanifold $\mathcal{N} \subset \mathcal{M}$ consisting of all sets Ω which are the union of disjoint balls

$$\Omega = \cup_i B_{R_i}(X_i),$$

where the centers $\{X_i\}_i$ and the radii $\{R_i\}_i$ are variable. Hence $\mathcal{N}$ can be identified with an open subspace of the hypersurface $\{\mathbf{Y} = \{R_i, X_i\}_i \in \mathbb{R}_+ \times \mathbb{R}^3 | \frac{4\pi}{3} \sum_i R_i^3 = \rho\}$ in $\mathbb{R}^{4N}$, where N is the number and $i = 1, \cdots, N$ an enumeration of the particles. The tangent space can be identified with the hyperplane

$$T_\mathbf{Y}\mathcal{N} = \left\{\mathbf{Z} = \{V_i, \xi_i\}_i \in \mathbb{R} \times \mathbb{R}^3 | \sum_i R_i^2 V_i = 0\right\} \subset \mathbb{R}^{4N},$$

such that V_i describes the rate of change of the radius of particle i and ξ_i the rate of change of its center.

The restriction of the metric tensor can be expressed as

$$g_\mathbf{Y}(\mathbf{Z}^1, \mathbf{Z}^2) = \int_{\mathbb{R}^3} \nabla w^1 \cdot \nabla w^2 \, dx,$$

where the function w^α solves

$$-\Delta w^\alpha = 0 \qquad \text{in } \mathbb{R}^3 \setminus \cup_i \partial B_{R_i}(X_i),$$
$$[\nabla w^\alpha \cdot \vec{n}] = V_i^\alpha + \xi_i^\alpha \cdot \vec{n} \quad \text{on } \partial B_{R_i}(X_i).$$

For the following it will be convenient to split the metric tensor into the radial and shift part respectively. We write

$$w = u + \phi$$

where u and ϕ are harmonic in- and outside the particles and where

$$\begin{aligned}
[\nabla u \cdot \vec{n}] &= V_i & \text{on } \partial B_{R_i}(X_i), \\
[\nabla \phi \cdot \vec{n}] &= \xi_i \cdot \vec{n} & \text{on } \partial B_{R_i}(X_i).
\end{aligned} \tag{6}$$

It turns out to be notationally convenient to consider the normalized energy $E = E_{surf} + \gamma E_{nl}$, where

$$E_{surf} = \frac{1}{2}\mathcal{H}^2(\partial\Omega) = 4\pi \sum_i \frac{R_i^2}{2}$$

and

$$E_{nl} = \frac{3}{2} \int_{\mathbb{R}^3} |\nabla\mu|^2 \, dx = \frac{3}{2} \sum_i \int_{B_{R_i}(X_i)} \mu \, dx$$

with $\mu = (-\Delta)^{-1}\chi_{\cup B_{R_i}}$. We obtain the differentials of the energies in the direction of a tangent vector $\tilde{\mathbf{Z}} = \{\tilde{V}_i, \tilde{\xi}_i\}_i$ as

$$\langle DE_{surf}, \tilde{\mathbf{Z}}\rangle = 4\pi \sum_i R_i \tilde{V}_i \quad \text{and} \quad \langle DE_{nl}, \tilde{\mathbf{Z}}\rangle = \frac{3}{2} \sum_i \int_{\partial B_{R_i}(X_i)} \mu\big(\tilde{V}_i + \tilde{\xi}_i \cdot \vec{n}\big) \, dS.$$

We will see in Section 2.2 that both, $g_{\mathbf{Y}}(\mathbf{Z}, \tilde{\mathbf{Z}})$ and $\langle DE_{nl}, \tilde{\mathbf{Z}} \rangle$, can be expressed explicitly in terms of $\{R_i, X_i\}_i$. For the moment we just state once more the gradient flow equation. For any $t \geq 0$ we chose $\mathbf{Z}(t)$ such that

$$g_{\mathbf{Y}}(\mathbf{Z}, \tilde{\mathbf{Z}}) = -\langle DE, \tilde{\mathbf{Z}} \rangle = -4\pi \sum_i R_i \tilde{V}_i - \gamma \frac{3}{2} \sum_i \int_{\partial B_{R_i}(X_i)} \mu \left(\tilde{V}_i + \tilde{\xi}_i \cdot \vec{n} \right) dS \quad (7)$$

for all $\tilde{\mathbf{Z}} \in T_{\mathbf{Y}} \mathcal{N}$. We can expect that if initial data $\{R_i(0), X_i(0)\}$ are given such that particles do not overlap, a smooth solution to (7) exists at least for short times. If a particle disappears the evolution is not smooth; we can, however, extend the solution continuously by just starting again with the new configuration. Our evolution cannot be further extended when two or more particles collide. We cannot completely exclude such an event a priori. However, as we will see below, one part of the nonlocal energy is given by $\sum_i \sum_{j \neq i} \frac{R_i^3 R_j^3}{|X_i - X_j|}$, which again shows that this part of the energy prefers uniformly distributed particles. If the energy is initially bounded, it remains bounded for all times as long as a solution exists. Hence, centers X_i and X_j cannot come arbitrarily close unless the particles become very small at the same time.

In the next Section 2.2 we solve the gradient flow equation. The main idea is that we can solve the equations for the potentials by superposition of suitable monopoles. We will see that the leading order terms in the equations differ, depending on whether the domain covered by the particles is larger or smaller than the well-known screening length that describes the effective interaction range of particles. In Section 2.3 we state the approximate equations for the gradient flow, first in the simplest case where the screening length is much larger than the system size, and second in the case in which the system size is of the order of the screening length. Those equations are the starting point for our numerical simulations. In Section 2.4 we derive the corresponding mean-field models which arise if one passes to a description with densities and in Section 3 we identify stationary states. Finally, in Section 4 we present results of numerical simulations of the monopole approximation.

2.2. **Solution by monopoles.** In this section we explicitly give the solution of the gradient flow equation based on the fact that we can solve the equations for the respective potentials in the metric tensor and for the nonlocal part of the energy explicitly by the superposition of monopoles.

The relevant length scales and parameters in our system are the following. We assume that initially we have a uniform distribution of particles contained in the box $(0, L)^3$. This property will not be conserved by the evolution but within the typical time scale particles remain in a box of order of size L.

We denote by $\frac{1}{d^3}$ the number density of particles, such that d is the typical distance of one particle to its nearest neighbor, and we call $\mathcal{R}$ the typical size of the radii of the particles. We are interested in the case that the A-phase has small volume fraction and hence we always assume that

$$\varepsilon := \frac{\mathcal{R}^3}{d^3} \ll 1. \quad (8)$$

It is well-known and it will also become apparent in the computations below that the crucial intrinsic length scale in diffusional interactions is the so-called screening length

$$L_{sc} = \left(\frac{d^3}{\mathcal{R}} \right)^{1/2}, \quad (9)$$

which describes the effective range of particle interactions. The following heuristic analysis shows that the leading order dynamics significantly differ, depending on whether $L \ll L_{sc}$ or whether $L \sim L_{sc}$.

2.2.1. *The energy.* In a first step we express the energy in terms of $\{R_i, X_i\}_i$, which is trivial for the surface energy but also simple for the nonlocal energy.

Indeed, the solution of $-\Delta\mu = \chi$ is given by $\mu = \sum_i \mu_i$, where

$$\mu_i(x) = \begin{cases} -\frac{|x-X_i|^2}{6} + \frac{R_i^2}{2} & : \quad \text{in } B_{R_i}(X_i) \\ \frac{R_i^3}{3|x-X_i|} & : \quad \text{outside } B_{R_i}(X_i) \end{cases}.$$

Thus we find, using the mean-value theorem for μ_j in B_{R_i} for $j \neq i$,

$$\begin{aligned}
E_{nl}(\mathbf{Y}) &= \frac{3}{2} \int_{\mathbb{R}^3} |\nabla\mu|^2 \, dx \\
&= \frac{3}{2} \sum_i \int_{B_{R_i}(X_i)} \mu \, dx \\
&= \frac{3}{2} \Big(\sum_i \int_{B_{R_i}(X_i)} \mu_i \, dx + \sum_i \int_{B_{R_i}(X_i)} \sum_{j \neq i} \mu_j \, dx \Big) \\
&= \frac{3}{2} \Big(\sum_i \int_{B_{R_i}(X_i)} \mu_i \, dx + \sum_i \sum_{j \neq i} \frac{4\pi}{3} R_i^3 \mu_j(X_i) \Big) \\
&= \frac{3}{2} \Big(\frac{8\pi}{15} \sum_i R_i^5 + \frac{4\pi}{9} \sum_i \sum_{j \neq i} \frac{R_i^3 R_j^3}{|X_i - X_j|} \Big) \\
&= 4\pi \Big(\sum_i \frac{R_i^5}{5} + \frac{1}{6} \sum_i \sum_{j \neq i} \frac{R_i^3 R_j^3}{|X_i - X_j|} \Big).
\end{aligned} \tag{10}$$

Hence, the differential of the energy $E = 4\pi \sum_i \frac{R_i^2}{2} + \gamma E_{nl}$ is given by

$$\begin{aligned}
\frac{1}{4\pi} \langle DE(\mathbf{Y}), \tilde{\mathbf{Z}} \rangle &= \sum_i R_i \tilde{V}_i + \gamma \sum_i R_i^4 \tilde{V}_i + \gamma \sum_i \sum_{j \neq i} \frac{R_i^2 R_j^3}{|X_i - X_j|} \tilde{V}_i \\
&\quad - \frac{\gamma}{3} \sum_i \sum_{j \neq i} \frac{R_i^3 R_j^3}{|X_i - X_j|^2} \frac{(X_i - X_j)}{|X_i - X_j|} \cdot \tilde{\xi}_i.
\end{aligned} \tag{11}$$

We can now compare the order of size of the different terms. First notice that in order that surface and nonlocal energy balance, the parameter γ has to be of size of order $\mathcal{R}^{-3}$ which we assume from now on.

Furthermore, in what follows, we approximate sums by the corresponding integral, i.e. $\sum_i \frac{1}{|x-X_i|} \sim \frac{1}{d^3} \int_{B_L(0)} \frac{1}{|x|} \sim \frac{L^2}{d^3}$, and we find that $\sum_{j \neq i} \frac{R_i^3 R_j^3}{|X_i - X_j|}$ has size of order $\mathcal{R}^6 \frac{L^2}{d^3}$. This is smaller than $\mathcal{R}^5$, the order of size of R_i^5, if $\frac{\mathcal{R}}{d^3} L^2 \ll 1$ or, in view of (9), if $L \ll L_{sc}$.

Equivalently, we can neglect the last two terms on the right hand side of (11) compared to the first two if $L \ll L_{sc}$. If, however, $L \sim L_{sc}$, all terms are of the same order of size.

2.2.2. *The metric tensor.* In this section we compute the metric tensor for given $\mathbf{Z} = \{V_i, \xi_i\}_i$ solving the equations for the potential $w = u + \phi$ respectively by

superposition of single particle solutions. Recall that $g_{\mathbf{Y}}(\mathbf{Z}, \mathbf{Z}) = \int_{\mathbb{R}^3} |\nabla u|^2 \, dx + 2 \int_{\mathbb{R}^3} \nabla u \cdot \nabla \phi \, dx + \int_{\mathbb{R}^3} |\nabla \phi|^2 \, dx$, where u and ϕ are given by (6).

One easily verifies that in case of a single particle $B_{R_i}(X_i)$ the solutions of problem (6) are given by

$$
u_i(x) = \begin{cases} -\frac{R_i^2 V_i}{|x - X_i|} & : \quad |x - X_i| \geq R_i \\ -R_i V_i & : \quad |x - X_i| \leq R_i \end{cases},
$$

$$
\phi_i(x) = \begin{cases} -\frac{R_i^3}{3|x - X_i|^3}(x - X_i) \cdot \xi_i & : \quad |x - X_i| \geq R_i \\ -\frac{1}{3}(x - X_i) \cdot \xi_i & : \quad |x - X_i| \leq R_i \end{cases}.
$$

Hence, for a system with N particles the potentials are given by

$$
u(x) := \sum_i u_i(x) \qquad \text{and} \qquad \phi(x) := \sum_i \phi_i(x).
$$

We first observe that

$$
\begin{aligned}
\int_{\mathbb{R}^3} |\nabla u|^2 \, dx &= \sum_i \int_{\mathbb{R}^3} |\nabla u_i|^2 \, dx + \sum_i \sum_{j \neq i} \int_{\mathbb{R}^3} \nabla u_i \cdot \nabla u_j \, dx \\
&= -\sum_i \int_{\partial B_{R_i}(X_i)} [\nabla u_i \cdot \vec{n}] u_i \, dS \\
&\quad - \sum_i \int_{\partial B_{R_i}(X_i)} [\nabla u_i \cdot \vec{n}] \sum_{j \neq i} u_j \, dS.
\end{aligned}
\tag{12}
$$

Now $[\nabla u_i \cdot \vec{n}] = V_i$ is constant on $\partial B_{R_i}(X_i)$ and u_j is harmonic in $B_{R_i}(X_i)$. Hence, the mean value theorem for harmonic functions implies $\int_{\partial B_{R_i}(X_i)} [\nabla u_i \cdot \vec{n}] \sum_{j \neq i} u_j \, dS = \sum_{j \neq i} V_i 4\pi R_i^2 u_j(X_i)$, and we arrive at

$$
\int_{\mathbb{R}^3} |\nabla u|^2 \, dx = 4\pi \sum_i R_i^3 V_i^2 + 4\pi \sum_i \sum_{j \neq i} V_i V_j \frac{R_i^2 R_j^2}{|X_i - X_j|}.
\tag{13}
$$

We compare the order of the first and second term in (13) respectively, as we did for the energy in Section 2.2.1. Keeping in mind that the number of particles is of order $\frac{L^3}{d^3}$, we find that the first term is of size of order $\frac{L^3}{d^3} \mathcal{R}^3 \mathcal{V}_R^2$, where $\mathcal{V}_R$ denotes the order of size of the velocities of the radii. Again approximating sums by integrals, the order of size of the second term is $\frac{L^3}{d^3} \mathcal{V}_R^2 \mathcal{R}^4 \frac{L^2}{d^3}$. Hence, the first term dominates if and only if $L^2 \ll \frac{d^3}{\mathcal{R}}$, that is, again, if the box size is much smaller than the screening length.

Similarly as in (12) we compute

$$\int_{\mathbb{R}^3} |\nabla \phi|^2 \, dx = \sum_i \int_{\mathbb{R}^3} |\nabla \phi_i|^2 \, dx + \sum_i \sum_{j \neq i} \int_{\mathbb{R}^3} \nabla \phi_i \cdot \nabla \phi_j \, dx$$

$$= -\sum_i \int_{\partial B_{R_i}(X_i)} [\nabla \phi_i \cdot \vec{n}] \phi_i \, dS$$

$$-\sum_i \int_{\partial B_{R_i}(X_i)} [\nabla \phi_i \cdot \vec{n}] \sum_{j \neq i} \phi_j \, dS$$

$$= \sum_i \tfrac{4}{3} \pi R_i^3 \fint_{\partial B_{R_i}(X_i)} |\xi_i \cdot \vec{n}|^2 \, dS$$

$$-\sum_i \int_{\partial B_{R_i}(X_i)} \xi_i \cdot \vec{n} \sum_{j \neq i} \phi_j \, dS.$$

Here and in the following we use the notation $\fint_{\partial B_{R_i}} := \frac{1}{4\pi R_i^2} \int_{\partial B_{R_i}}$ for mean values. It is easily calculated, for instance by using polar coordinates, that

$$\fint_{\partial B_{R_i}(X_i)} |\xi_i \cdot \vec{n}|^2 \, dS = \fint_{S^2} |\xi_i \cdot \vec{n}|^2 \, dS = \frac{1}{3} |\xi_i|^2$$

and thus

$$\int_{\mathbb{R}^3} |\nabla \phi|^2 \, ds = \frac{4\pi}{9} \sum_i R_i^3 |\xi_i|^2 - \sum_i \int_{\partial B_{R_i}(X_i)} \xi_i \cdot \vec{n} \sum_{j \neq i} \phi_j \, dS. \qquad (14)$$

The second term is computed with the help of Gauss' theorem and again the mean value theorem,

$$\sum_i \sum_{j \neq i} \int_{\partial B_{R_i}(X_i)} \xi_i \cdot \vec{n} \, \phi_j \, dS = \sum_i \sum_{j \neq i} \int_{B_{R_i}(X_i)} \xi_i \cdot \nabla \phi_j \, dx$$

$$= \frac{4\pi}{9} \sum_i \sum_{j \neq i} \left(\frac{3 R_i^3 R_j^3}{|X_i - X_j|^5} (X_i - X_j) \cdot \xi_i (X_i - X_j) \cdot \xi_j - \frac{R_i^3 R_j^3}{|X_i - X_j|^3} \xi_i \cdot \xi_j \right).$$

It turns out to be of higher order than the diagonal term. Indeed, the latter is of order $\frac{L^3}{d^3} \mathcal{R}^3 \mathcal{V}_X^2$, where $\mathcal{V}_X$ is the order of size of the midpoint velocities, and the order of the ratio of the former and this term can be estimated as before by $\frac{\mathcal{R}^3}{d^3} \sum_{j \neq i} \frac{1}{|X_i - X_j|} \sim \varepsilon \ln(1/\varepsilon)$.

Finally, for the mixed term of the metric tensor we find

$$\int_{\mathbb{R}^3} \nabla u \cdot \nabla \phi \, dx = \sum_i \int_{\mathbb{R}^3} \nabla u_i \cdot \nabla \phi \, dx$$

$$= -\sum_i \int_{\partial B_{R_i}(X_i)} V_i \phi \, dS$$

$$= -\sum_i V_i \int_{\partial B_{R_i}(X_i)} \sum_{j \neq i} \phi_j \, dS$$

$$= 4\pi \sum_i \sum_{j \neq i} \frac{R_j^3 R_i^2}{3|X_i - X_j|^3} V_i (X_i - X_j) \cdot \xi_j.$$

In the last equalities we used that $\int_{\partial B_{R_i}(X_i)} \phi_i \, dS = -\frac{R_i}{3} \int_{\partial B_{R_i}(X_i)} \xi_i \cdot \vec{n} \, dS = 0$ and, as in the derivation of (13), that ϕ_j is harmonic in $B_{R_i}(x_i)$ for $j \neq i$.

To summarize we obtain

$$
\begin{aligned}
g_{\mathbf{Y}}(\mathbf{Z}, \mathbf{Z}) = {} & 4\pi \sum_i R_i^3 V_i^2 + 4\pi \sum_i R_i^3 \frac{1}{9} |\xi_i|^2 \left(1 + \mathcal{O}\big(\varepsilon \ln \frac{1}{\varepsilon}\big) \right) \\
& + 4\pi \sum_i \sum_{j \neq i} \frac{R_i^2 R_j^2}{|X_i - X_j|} V_i V_j \\
& + 8\pi \sum_i \sum_{j \neq i} \frac{R_j^3 R_i^2}{3 |X_i - X_j|^3} V_i (X_i - X_j) \cdot \xi_j,
\end{aligned}
\tag{15}
$$

and the diagonal terms dominate if $L \ll L_{sc}$.

2.3. Leading order approximations.

We now set up an approximation of the gradient flow, keeping only the leading order terms in the energy and the metric tensor respectively. This will be the starting point for numerical simulations whose results we present in Section 4 below. As we have seen, there are two regimes of interest. The first one is the dilute case, where the system size is much smaller than the screening length.

2.3.1. *Case I: $L \ll L_{sc}$.* In case $L \ll L_{sc}$ we obtain, in view of (10) and the subsequent discussion, that

$$
E(\mathbf{Y}) \sim 4\pi \left(\sum_i \frac{R_i^2}{2} + \gamma \sum_i \frac{R_i^5}{5} \right),
\tag{16}
$$

whereas the metric tensor can be approximated due to (15) by

$$
g_{\mathbf{Y}}(\mathbf{Z}, \mathbf{Z}) \sim 4\pi \sum_i R_i^3 \left(V_i^2 + \frac{1}{9} |\xi_i|^2 \right).
$$

The gradient flow equation $g_{\mathbf{Y}}(\mathbf{Z}, \tilde{\mathbf{Z}}) + \langle DE(\mathbf{Y}), \tilde{\mathbf{Z}} \rangle = 0$ reads

$$
\sum_i R_i^3 \left(V_i \tilde{V}_i + \frac{1}{9} \xi_i \cdot \tilde{\xi}_i \right) + \sum_i R_i \tilde{V}_i + \gamma \sum_i R_i^4 \tilde{V}_i = 0
$$

for all $\{\tilde{V}_i, \tilde{\xi}_i\}$ in the tangent space. This is equivalent to

$$
\sum_i R_i^3 \big(V_i \tilde{V}_i + \frac{1}{9} \xi_i \cdot \tilde{\xi}_i \big) + \sum_i R_i \tilde{V}_i + \gamma \sum_i R_i^4 \tilde{V}_i = \lambda \sum_i R_i^2 \tilde{V}_i
$$

for all $\{\tilde{V}_i, \tilde{\xi}_i\} \in \mathbb{R}^{4N}$, where λ is a Lagrange multiplier to ensure $\sum_i R_i^2 V_i = 0$.

Consequently, we obtain for the direction of steepest descent that

$$
V_i = \frac{1}{R_i^2} \big(\lambda R_i - 1 - \gamma R_i^3 \big) \qquad \text{and} \qquad \xi_i = 0,
\tag{17}
$$

where

$$
\lambda = \frac{\sum_{i : R_i > 0} 1 + \gamma \frac{3\rho}{4\pi}}{\sum_i R_i}.
\tag{18}
$$

2.3.2. *Case II: $L \sim L_{sc}$.* With the same procedure as above we infer from (11) and (15) that V_i solves the linear system of equations

$$
\begin{gathered}
R_i^2 V_i + R_i \sum_{j \neq i} \frac{R_j^2}{|X_i - X_j|} V_j + 1 + \gamma R_i^3 + \gamma R_i \sum_{j \neq i} \frac{R_j^3}{|X_i - X_j|} \\
= \lambda R_i - \sum_{j \neq i} \frac{R_j^3 R_i}{3|X_i - X_j|^3} (X_i - X_j) \cdot \xi_j,
\end{gathered}
\tag{19}
$$

where λ is such that $\sum_i R_i^2 V_i = 0$, and we get the nontrivial evolution equation

$$
\xi_i = \sum_{j \neq i} \frac{3\gamma R_j^3 + R_j^2 V_j}{|X_i - X_j|^3} (X_i - X_j)
\tag{20}
$$

for the centers. Notice that (20) implies that $\mathcal{V}_X$ is of order L/d^3. Using this in (19), we see that the last term on the right hand side is of order $\mathcal{R}^4 L^2/d^6 = \varepsilon (L/L_{sc})^2$ and can be neglected compared to the other terms, which are of order 1. We finally obtain that the evolution of the radii is to leading order governed by

$$
R_i^2 V_i + R_i \sum_{j \neq i} \frac{R_j^2}{|X_i - X_j|} V_j + 1 + \gamma R_i^3 + \gamma R_i \sum_{j \neq i} \frac{R_j^3}{|X_i - X_j|} = \lambda R_i.
\tag{21}
$$

2.4. **Mean-field models.** In this section we derive mean-field models which arise if one passes from the discrete setting of finitely many particles to a description with densities. Our derivation is purely formal and starts from (17) and (20)–(21) respectively. A rigorous derivation from the full model in the spirit of [9] seems feasible under some assumptions on the distribution of particles. This is, however, not within the scope of this paper.

For the derivation of mean-field models we need to go over to suitably rescaled variables. First we recall the relevant parameters and length scales in our system. We denote by N the total number of particles, by $\frac{1}{d^3}$ the number density, and by $\mathcal{R}$ the typical particle radius. Our system size, that is the area covered with particles, is then $L^3 \sim N d^3$. The crucial intrinsic length scale is the screening length $L_{sc} \sim (d^3/\mathcal{R})^{1/2}$. Note that these quantities are in general time dependent. As introduced here they refer to the initial configuration and we derive the mean-field models for finite times in which these length scales remain of the same order.

Recall also that in order to balance surface and nonlocal energy our parameter γ must be of order $\mathcal{R}^{-3}$. Hence, we set from now on

$$
\tilde{\gamma} := \gamma \mathcal{R}^3.
$$

2.4.1. *Case I: $L \ll L_{sc}$.* We start with the simple case $L \ll L_{sc}$. In view of (17) we measure the time in which radii change in units of $\mathcal{R}^3$, that is, we introduce the new time scale $\tau = t/\mathcal{R}^3$. Since $\xi_i = 0$ in the dilute regime, it suffices to consider the distribution of particle radii. Let

$$
r_i(\tau) = \frac{R_i(t)}{\mathcal{R}}, \qquad v_i := \mathcal{R}^2 V_i,
\tag{22}
$$

and define

$$
\int \zeta \, \nu_\tau(dr) := \frac{1}{N} \sum_i \zeta(r_i),
$$

where $\zeta \in C_0^\infty((0, \infty))$. Then, using (17), we find

$$\frac{d}{d\tau} \int \zeta \, \nu_t(dr) = \frac{1}{N} \sum_i \partial_r \zeta \, v_i$$

$$= \frac{1}{N} \sum_i \partial_r \zeta \frac{1}{r_i^2} \left(\tilde{\lambda} r_i - 1 - \tilde{\gamma} r_i^3 \right) \tag{23}$$

$$= \int \partial_r \zeta \frac{1}{r^2} \left(\tilde{\lambda} r - 1 - \tilde{\gamma} r^3 \right) \nu_\tau(dr),$$

where $\tilde{\lambda} = \lambda \mathcal{R}$ is such that $\int r^3 \, \nu_t(dr) \equiv \frac{3\rho}{4\pi N} =: \tilde{\rho}$. Equation (23) just means that ν_t satisfies

$$\partial_\tau \nu_\tau + \partial_r \left(\frac{1}{r^2} \left(\tilde{\lambda} r - 1 - \tilde{\gamma} r^3 \right) \nu_\tau \right) = 0 \tag{24}$$

with

$$\tilde{\lambda}(\tau) = \frac{\int \nu_\tau(dr) + \tilde{\gamma}\tilde{\rho}}{\int r \nu_\tau(dr)}$$

in the sense of distributions.

For $\tilde{\gamma} = 0$ we recover the LSW-theory for coarsening of particles. For $\tilde{\gamma} > 0$ the additional term $\tilde{\gamma} \sum_i \frac{R_i^5}{5}$ in the energy prevents coarsening and hence the long-time behavior of (24) is different from the one for $\tilde{\gamma} = 0$. Indeed, while the energy (16) together with the volume constraint has no stationary point for $\tilde{\gamma} = 0$, we will see in Section 3 below, that (16) has a unique global minimizer for $\tilde{\gamma} > 0$ which is also the only stationary point with respect to an appropriate topology.

2.4.2. *Case II: $L \sim L_{sc}$.* We assume now that $L \sim L_{sc} = \left(\frac{d^3}{\mathcal{R}} \right)^{1/2}$. In addition to r_i and v_i as in (22) we also introduce

$$x_i(\tau) := \frac{X_i(t)}{L_{sc}} \qquad \text{and} \qquad \psi_i := \frac{d^3}{L_{sc}} \xi_i. \tag{25}$$

Now we define the joint distribution of particle centers and radii via

$$\int \zeta \, \nu_\tau(dx \, dr) := \frac{1}{N} \sum_i \zeta(x_i, r_i)$$

for $\zeta \in C_0^\infty(\mathbb{R}^3 \times (0, \infty))$. We are going to derive that ν_t satisfies the following system of equations in a distributional sense:

$$\partial_\tau \nu_\tau + \partial_r \left(\frac{1}{r^2} \left(r\bar{u} - 1 - \tilde{\gamma} \left(r^3 + rK(x) \right) \right) \nu_\tau \right) + \varepsilon \, \mathrm{div}_x \left(3(\nabla \bar{u} - \tilde{\gamma} \nabla K(x)) \nu_\tau \right) = 0, \tag{26}$$

where ε is the volume fraction (recall (8)),

$$K(x) = \int \frac{s^3}{|x - y|} \nu_\tau(dy \, ds) \tag{27}$$

(notice that the integral is finite since ν_τ has finite support in the x-variable) and $\bar{u} = \bar{u}(x, \tau)$ satisfies

$$-\frac{1}{4\pi} \Delta_x \bar{u} + \bar{u} \int_0^\infty r \nu_\tau(dr) - \int_0^\infty \nu_\tau(dr) - \tilde{\gamma} \left(\int_0^\infty r^3 \, \nu_\tau(dr) + K(x) \int_0^\infty r \nu_\tau(dr) \right) = 0 \tag{28}$$

in $\mathbb{R}^3$ for each τ.

Indeed, we first recall (25), to find

$$\frac{d}{d\tau} \int \zeta \, \nu_\tau (dx \, dr) = \frac{1}{N} \sum_i \big(\varepsilon \nabla \zeta \cdot \psi_i + \partial_r \zeta v_i\big). \tag{29}$$

Equation (20) gives

$$
\begin{aligned}
\psi_i &= 3 \frac{d^3}{L_{sc}} \sum_{j \neq i} \Big(\tilde\gamma \frac{R_j^3}{\mathcal{R}^3} + R_j^2 V_j\Big) \frac{X_i - X_j}{|X_i - X_j|^3} \\
&= 3 \frac{d^3}{L_{sc}^3} \sum_{j \neq i} \big(\tilde\gamma r_j^3 + r_j^2 v_j\big) \frac{x_i - x_j}{|x_i - x_j|^3} \\
&= 3 \tilde\gamma \frac{1}{N} \sum_{j \neq i} r_j^3 \frac{x_i - x_j}{|x_i - x_j|^3} + \frac{3}{N} \sum_{j \neq i} r_j^2 v_j \frac{x_i - x_j}{|x_i - x_j|^3} \\
&= -3\tilde\gamma \nabla K(x_i) + 3 \nabla \bar{u}(x_i).
\end{aligned} \tag{30}
$$

where $\bar{u}(x)$ (neglecting in the notation the dependence on t) is given by

$$- \bar{u}(x) := \mathcal{R} \Big(\frac{1}{L_{sc}} \sum_{j \neq i} \frac{r_j^2 v_j}{|x - x_j|} - \lambda\Big) = \frac{1}{N} \sum_{j \neq i} \frac{r_j^2 v_j}{|x - x_j|} - \lambda \mathcal{R}. \tag{31}$$

Then (21) reads

$$
\begin{aligned}
R_i^2 V_i &= \frac{R_i \bar{u}(x_i)}{\mathcal{R}} - 1 - \gamma \Big(R_i^3 + R_i \frac{1}{L_{sc}} \sum_{j \neq i} \frac{R_j^3}{|x_i - x_j|}\Big) \\
&= r_i \bar{u}(x_i) - 1 - \tilde\gamma \Big(r_i^3 + r_i K(x_i)\Big),
\end{aligned} \tag{32}
$$

where we used (27) in the last step as well as the fact $\mathcal{R}N = L_{sc}$, which is due to $L = L_{sc}$. Inserting (32) into (31), we obtain

$$
\begin{aligned}
-\bar{u}(x) &= \frac{\mathcal{R}}{L_{sc}} \sum_{j \neq i} \frac{r_j \bar{u}(x_j) - 1 - \tilde\gamma(r_j^3 + r_j K(x_j))}{|x - x_j|} - \lambda \mathcal{R} \\
&= \int \frac{r \bar{u}(y) - 1 - \tilde\gamma(r^3 + r K(y))}{|x - y|} \nu_\tau (dy \, dr) - \lambda \mathcal{R}.
\end{aligned}
$$

If we take the Laplacian in the last equation, we obtain (28). Finally, (26) follows from (29), (30) and (32).

3. **Stationary points of the energy.** In this section we investigate the stationary states of the energies. Since we are interested in configurations with a large number of particles, we consider the continuous case. As we will argue later, in our setting stationary points only exist in the dilute case, so we first concentrate on this. For notational convenience we rename $\tilde\rho$ and $\tilde\gamma$ by ρ and γ again. Thus, let ν be a measure on $(0, \infty)$ such that

$$\rho = \frac{4\pi}{3} \int_0^\infty r^3 \, \nu(dr)$$

is fixed. The energy of ν is

$$E(\nu) = 4\pi \int \Big(\frac{r^2}{2} + \gamma \frac{r^5}{5}\Big) \nu(dr).$$

Lemma 3.1. *Among measures ν with the fixed volume ρ the energy E is minimized at $\nu = \frac{3\rho}{4\pi\, r_*^3}\delta_{r_*}$, where $r_* = (\frac{5}{4\gamma})^{1/3}$.*

Proof. Let μ be a measure so that

$$\mu(dr) = r^3 \nu(dr).$$

Then

$$E(\nu) = 4\pi \int \left(\frac{1}{2r} + \gamma \frac{r^2}{5} \right) \mu(dr)$$

Since the integrand is convex, by Jensen's inequality we have

$$E(\nu) \geq 3\,\rho \left(\frac{1}{2\bar{r}} + \gamma \frac{\bar{r}^2}{5} \right) \tag{33}$$

where $\bar{r} = \frac{4\pi}{3\rho} \int r\, \mu(dr)$ is the average of r under μ. Note that equality in (33) holds only when $\mu = \frac{3\rho}{4\pi}\delta_{\bar{r}}$. In this case $\nu = \frac{3\rho}{4\pi\bar{r}^3}\delta_{\bar{r}}$. So it suffices to minimize E among such measures and, since

$$E\left(\frac{\rho}{\bar{r}^3}\delta_{\bar{r}} \right) = 3\frac{\rho}{\bar{r}^3}\left(\frac{\bar{r}^2}{2} + \gamma \frac{\bar{r}^5}{5} \right) = 3\rho\left(\frac{1}{2\bar{r}} + \gamma \frac{\bar{r}^2}{5} \right)$$

is convex in $\bar{r}$, E is minimized at $\frac{3\rho}{4\pi r_*^3}\delta_{r_*}$, with $r_* = \left(\frac{5}{4\gamma} \right)^{1/3}$. $\qquad\square$

Next we investigate stationary points of E. The notion of stationary points depends on the variations and hence the topology one uses in the space of measures. The coarsest topology is the one induced by the Wasserstein distance, which metrizes the weak topology of measures. In one dimension the Wasserstein distance is easy to compute. Let

$$Z_1(r) = \nu_1([r, \infty)), \ \ Z_2(r) = \nu_2([r, \infty))$$

be the radius distributions of the measures ν_1 and ν_2 and denote by $r_1(z), r_2(z)$ their right-continuous inverses. The L^p-Wasserstein distance between ν_1 and ν_2 is given by

$$\rho(\nu_1, \nu_2) := \|r_1 - r_2\|_p = \left(\int_0^\infty |r_1(z) - r_2(z)|^p\, dz \right)^{1/p}. \tag{34}$$

In the next lemma we show that the only stationary point of the energy with respect to the topology induced by the Wasserstein distance is the global minimizer identified in Lemma 3.1.

Lemma 3.2. *Let ν be a stationary point of E with respect to the topology induced by (34). Then $\nu = \frac{3\rho}{4\pi\, r_*^3}\delta_{r_*}$ and $r_* = \left(\frac{5}{4\gamma} \right)^{1/3}$.*

Proof. Let ν be a stationary point of E and $r = r(z)$ the right-continuous inverse of its distribution function as described above. We do not assume that ν is a finite measure, hence r might not have finite support. In terms of r the energy is given by

$$E(\nu) = 4\pi \int_0^\infty \frac{r^2(z)}{2} + \gamma \frac{r^5(z)}{5}\, dz =: \hat{E}(r).$$

The constraint $\frac{4\pi}{3} \int r^3 \nu(dr) = \rho$ corresponds to $\frac{4\pi}{3} \int r^3(z)\, dz = \rho$. We consider now so called inner variations, that is, we consider $r^\varepsilon(z) := r(z + \varepsilon\eta(z))$, where

$\eta \in C_0^\infty((0, \infty))$ is such that $\frac{4\pi}{3} \int_0^\infty r^\varepsilon(z)\, dz = \rho$. We find

$$\frac{d}{d\varepsilon} \hat{E}(r^\varepsilon)_{|\varepsilon=0} = \frac{d}{d\varepsilon}_{|\varepsilon=0} \int_0^\infty \left(\frac{r^{\varepsilon 2}}{2} + \gamma \frac{r^{\varepsilon 5}}{5} \right) dz$$

$$= -\int_0^\infty \left(\frac{r^2}{2} + \gamma \frac{r^5}{5} \right) \eta'(z)\, dz.$$

Furthermore, the volume constraint $\frac{4\pi}{3} \int_0^\infty r^{\varepsilon 3}(z)\, dz = \rho$ implies similarly that $\int_0^\infty r^3 \eta'(z)\, dz = 0$. Thus, in summary we find that

$$\int_0^\infty \left(\frac{r^2}{2} + \gamma \frac{r^5}{5} - \lambda r^3 \right) \psi'(z)\, dz = 0 \qquad (35)$$

for all $\psi \in C_0^\infty((0, \infty))$ and for some $\lambda \in \mathbb{R}$. Let $\{z_i\}, i \in I \subset \mathbb{N}$, be the set of discontinuity points of r (which is an at most countable set, since r is decreasing). With this notation we deduce from (35) after an integration by parts that

$$\int_0^\infty \left(r + \gamma r^4 - 3\lambda r^2 \right) \psi(z)\, dz$$

$$+ \sum_{i \in I} \left[\left(\frac{r^2}{2} + \gamma \frac{r^5}{5} - \lambda r^3 \right)(z_i) - \lim_{z \to z_i, z < z_i} \left(\frac{r^2}{2} + \gamma \frac{r^5}{5} - \lambda r^3 \right)(z) \right] \psi(z_i) = 0$$

for all $\psi \in C_0^\infty((0, \infty))$. It follows that r has to be piecewise constant, say $r(z) \equiv r_i \in [z_{i-1}, z_i)$ (with the convention that $z_0 = 0$), and r_i must be a zero of $f(r) := r + \gamma r^4 - 3\lambda r^2$ for some $\lambda \in \mathbb{R}$. Furthermore, we find

$$\frac{r_i^2}{2} + \gamma \frac{r_i^5}{5} - \lambda r_i^3 = \frac{r_{i-1}^2}{2} + \gamma \frac{r_{i-1}^5}{5} - \lambda r_{i-1}^3$$

for all $i \in I$. A simple calculation shows that this can only be true if $I = \{1\}$ and $r_1 = r_* = \left(\frac{5}{4\gamma} \right)^{1/3}$ and $r_2 = 0$. The point z_1, where r jumps, is determined by the volume constraint and hence given by $z_1 = \frac{3\rho}{4\pi\, r_*^3}$. $\qquad \square$

Remark 3.3. (The inhomogeneous case) It is in principle a very interesting question, how in the case $L \sim L_{sc}$ the additional inhomogeneous term in the energy,

$$\frac{1}{N^2} \sum_i r_i^3 \sum_{j \neq i} \frac{r_j^3}{|x_i - x_j|} = \int r^3 K(x)\, \nu(dx\, dr),$$

changes the configuration of stationary points. However, in our case there are no stationary states. This is due to the somewhat artificial setting, where we set particles in a bounded domain but solve the equations for the corresponding potentials in full space. From equation (20) for the evolution of particle centers we easily see that particles located at the boundary of our "cloud" of particles will be driven further outwards.

If instead we would confine particles and their corresponding potentials to a finite domain and impose periodic or Neumann boundary conditions we would obtain similar formulas for our approximate gradient flow equations and the mean-field models, but $\frac{1}{|x|}$ would be replaced by the corresponding Green's function. Then stationary states would be characterized by $K \equiv const$, which would imply a regular spacing the particles. Once K is constant, the term $\int r^3 K \nu(dx\, dr)$ is also constant due to the volume constraint. The remaining discussion of stationary points is then analogous to the dilute case.

From the discussion in the mean-field theory, Section 2.4.2, we know that the particle centers move on a slower time scale d^3 than the particle radii, which change on a time scale of order $\mathcal{R}^3$. Consequently, in our simulations the movement of particles is almost negligible compared to the evolution of the radii.

Remark 3.4. (The discrete setting) Naturally, the discrete case is somewhat different from the continuous one, since the number of particles is integer and we cannot reach any arbitrary fraction of particles. As argued in Remark 3.3 above, we can concentrate on the dilute case (17).

Let us first consider the situation from the point of view of the evolution. Our initial configuration consists of N particles with total volume $\rho = \sum_i \frac{4\pi}{3} R_i^3 \sim N \frac{4\pi \mathcal{R}^3}{3}$. Since during our evolution particles can only vanish, we consider stationary states with $N_1 \leq N$ particles. For any given N_1 there is a family of stationary states. First there is the trivial one, that is $R_i \equiv \hat{r}$ for all i and $\hat{r} = \frac{3\rho}{4\pi N_1}$. However, due to the discreteness of the problem there are now also stationary states with two different sizes of particles. For that let $\sigma := \frac{N_2}{N_1} \in (0, 1]$, where N_2 will be the number of particles with one radius r_1, whereas $N_1 - N_2$ will be the number of particles with another radius r_2. In view of (17) stationary states of the desired form are given by radii which are zeros of the function $f(r) := 1 + \gamma r^3 - \lambda r$ for some $\lambda \in \mathbb{R}$. There can be at most two different radii for which this is satisfied. We denote them by r_1 and r_2. To say that r_1 and r_2 are zeros of the function f for some λ is equivalent to requiring that $\frac{1}{r_1} + \gamma r_1^2 = \frac{1}{r_2} + \gamma r_2^2$ holds true. In order to satisfy the volume constraint, we must have $\sigma r_1^3 + (1-\sigma) r_2^3 = \frac{3\rho}{4\pi N_1} =: \beta$. Using the last equation to express r_2 by r_1 we find that $r_2^3 = \frac{\beta - \sigma r_1^3}{1-\sigma}$. Now the corresponding r_1 is determined as a zero of $g(r) := \frac{1}{r} + \gamma r^2 - \left(\frac{1-\sigma}{\beta - \sigma r^3}\right)^{1/3} - \gamma \left(\frac{\beta - \sigma r^3}{1-\sigma}\right)^{2/3}$. Since $\lim_{r \to 0} g(r) = +\infty$ and $\lim_{r \to \sigma^{-1/3}} g(r) = -\infty$ there is at least one solution. Thus we have a whole set of stationary states for given $N_1 \leq N$ which consist of two different sizes of particles. Due to the convexity of the energy they have higher energy than the stationary state where only one size is present and the size is given by $\hat{r} = \frac{3\rho}{4\pi N_1}$. This is true for fixed N_1. Of course, depending on the choice of parameters, it might be that a stationary state with two different sizes for one N_1 has lower energy than the trivial stationary state for a different given number of particles.

4. **Simulations.** For numerical simulation it is convenient to re-formulate (17) and (20)–(21) in terms of particle volumes and their velocities instead of radii. This has the advantage that the constraint of volume conservation becomes linear. For that let $W_i := R_i^3$ and $\omega_i := \frac{d}{dt} W_i$. The equations then read

$$\omega_i = 3(\lambda R_i - 1 - \gamma R_i^3) \qquad \text{and} \qquad \xi_i = 0 \tag{36}$$

with λ as in (18) in the dilute case, and

$$\omega_i + R_i \sum_{j \neq i} \frac{\omega_j}{|X_i - X_j|} + \lambda = -3 - 3\gamma R_i^3 - 3\gamma R_i \sum_{j \neq i} \frac{R_j^3}{|X_i - X_j|},$$

$$\xi_i = \sum_{j \neq i} \frac{3\gamma R_j^3 + \omega_j}{|X_i - X_j|^3}(X_i - X_j) \tag{37}$$
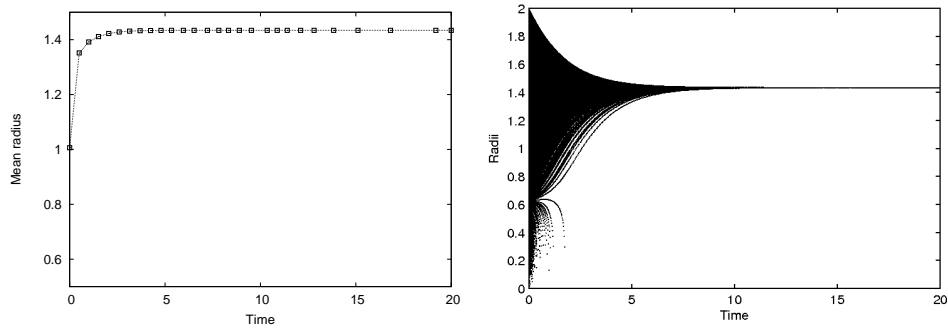
in case $L \sim L_{sc}$.

FIGURE 1. Example for an evolution of mean radius and all particle radii in the dilute case.

Initial N	Initial radii distribution	$(5/4\gamma)^{1/3}$	Final radius	Final N
1000	uniformly in $(0, 2)$	1.365	1.434	690
1000	uniformly in $(0.5, 1.5)$	1.365	1.202	742
1000	normally in $(0, 2)$	1.365	1.197	768
1000	normally in $(0.5, 1.5)$	1.365	1.115	846
2197	uniformly in $(0, 0.88)$	0.599	0.628	1529
4096	uniformly in $(0, 0.432)$	0.202	0.305	2886

TABLE 1. Results of simulated particle systems all within the same parameter region, but different radii distribution.

To simulate the behavior of our gradient flow model with these equations we set up a simple numerical scheme consisting of an Euler predictor and a trapezoidal rule corrector step. The latter is also used as error indicator and to determine – beside the influence of vanishing particles – a suitable step size. Particles are removed when they become too small, i.e. if $W_i < \delta \sum W_i/N$ where N denotes the current number of particles and δ is a user-defined tolerance. Under no circumstances we allow particle volumes to become negative.

At each time step the velocities of particle midpoints and volumes are computed via (36) and (37), respectively. While this is not much work in the first case, we have to solve a symmetric, indefinite, and dense linear system of size $N+1$ in the second case. Due to its potential structure, however, the product of the system matrix with an arbitrary vector can be computed in almost linear time by means of the Fast Multipole Method [7, 8]. This and the approximate weak diagonal dominance of the matrix enable us to efficiently apply a Krylov subspace method to solve (37) for large systems.

We start our simulations with a number of particles distributed regularly on a mesh in some box $(0, L)^3$. From the mesh size and (9) we obtain the value of the initial mean or typical radius in order that $L = L_{sc}$ is approximately fulfilled. We simulate the dilute and the full problem with the same radius distribution to be able to compare the results.

4.1. **Case I: $L \ll L_{sc}$.** For any distribution of radii which we consider in our simulations, uniformly or normally distributed in some interval about the initial mean radius or special as stated below, the system reaches a stationary state. As
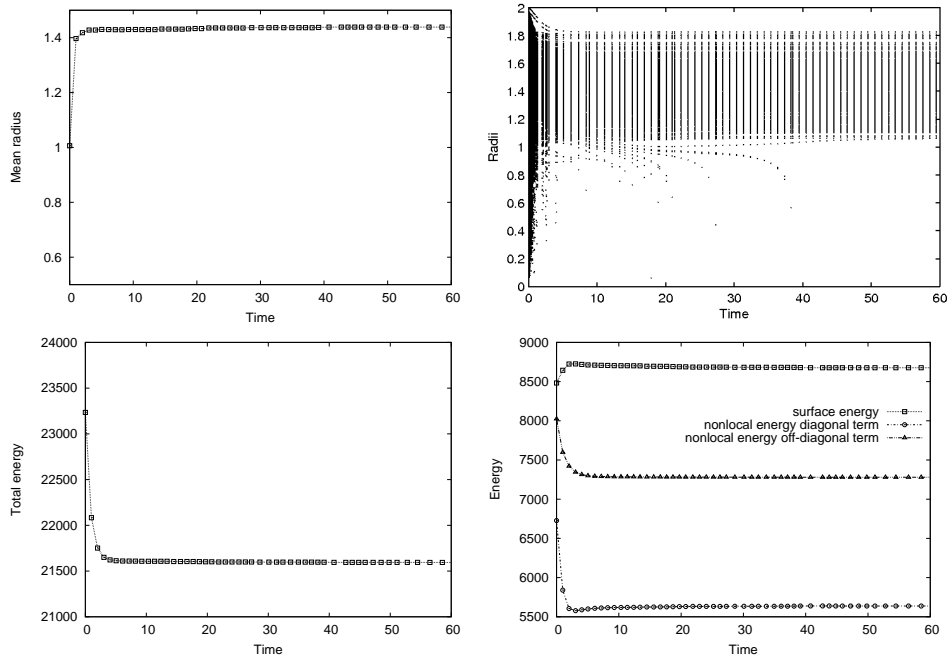
FIGURE 2. Evolution of mean radius, particle radii and energy in
the full problem; compare with Figure 1 where the same system in
the dilute case is shown.

expected from Remark 3.4 this final state is characterized by either all particles
having (almost) the same size or one of two radii with the condition stated there.
The latter case, however, only appears when we already start the simulation with
such a particle configuration; in general we arrive at a stationary state concentrated
in one size.

However, the computed stationary state is not the global minimizer derived in
Section 3, which, of course, might be infeasible due to the volume constraint and
integer number of particles. In general one cannot even say that it is close to or
approaches it when the number of particles grows. In fact, the computed state and
its difference from the predicted minimizer of the continuous case in terms of the
final radius depend on the actual distribution of the radii, as can be seen in Figure
1 and Table 1.

4.2. **Case II:** $L \sim L_{sc}$**.** As expected, the evolution of the full problem does not
reach a stationary state, i. e. a state in which all velocities are identically zero, since
particles drift out of the box. But the following two observations can be made, as
can be seen for instance in Figure 2. First of all, even though drifting can occur,
its influence on energy minimizing is distinguishable from that of radii evolution
and – as already stated in Remark 3.3 – can be neglected in case the value of L_{sc}
is not much smaller than the box size. Secondly and more important, one observes
that the total energy in principle tends towards a stationary value, as does the
mean particle radius. However, the final mean radius is in general not equal to that
from the same initial configuration evolving under the dilute equations. Another
difference is that in the full problem the particles do not tend to have equal size.

Instead, after a phase of vanishing and approaching it, all remaining particles have a radius in some interval about the final mean radius which is smaller than the initial radii interval, but whose size again seems to depend on the actual initial distribution.

REFERENCES

[1] N. Alikakos and G. Fusco, *Ostwald ripening for dilute systems under quasistationary dynamics*, Comm. Math. Phys., **238** (2003), 429–479.

[2] X. Chen, *The Hele-Shaw problem and area-preserving curve shortening motion*, Arch. Rat. Mech. Anal., **123** (1993), 117–151.

[3] X. Chen, X. Hong and F. Yi, *Existence, uniqueness and regularity of classical solutions of the Mullins-Sekerka problem*, Comm. PDE, **21** (1996), 1705–1727.

[4] R. Choksi, *Scaling laws in microphase separation of diblock copolymers*, J. Nonlinear Sci., **11** (2001), 223–236.

[5] S. Dai, B. Niethammer and R. L. Pego, *Crossover in coarsening rates for the monopole approximation of the Mullins-Sekerka model with kinetic drag*, Preprint, 2008.

[6] J. Escher and G. Simonett, *A center manifold analysis for the Mullins-Sekerka model*, J. Differential Equations, **143** (1998), 267–292.

[7] L. Greengard, "The Rapid Evaluation of Potential Fields in Particle Systems," MIT Press, Cambridge, Massachusetts, 1987.

[8] L. Greengard and V. Rokhlin, *A new version of the fast multipole method for the Laplace equation in three dimensions*, Acta Numerica, **6** (1997), 229–269.

[9] B. Niethammer and F. Otto, *Ostwald ripening: the screening length revisited*, Calc. Var. and PDE, **13** (2001), 33–68.

[10] Y. Nishiura and I. Ohnishi, *Some mathematical aspects of the microphase separation in diblock copolymers*, Physica D, **84** (1995), 31–39.

[11] T. Ohta and K. Kawasaki, *Equilibrium morphology of block copolymer melts*, Macromolecules, **19** (1986), 2621–2632.

[12] X. Ren and J. Wei, *On the multiplicity of solutions of two nonlocal variational problems*, SIAM J. Math. Anal., **31** (2000), 909–924.

[13] X. Ren and J. Wei, *Spherical solutions to a nonlocal free boundary problem from diblock copolymer morphology*, SIAM J. Math. Anal., **39** (2008), 1497–1535.

E-mail address: `niethammer@maths.ox.ac.uk`